PERGAMON

International Journal of Heat and Mass Transfer 45 (2002) 4401–4408

International Journal of HEAT and MASS TRANSFER

www.elsevier.com/locate/ijhmt

Experimental studies of combined heat transfer in turbulent mixed convection fluid flows in double-skin-façades

A. Zöllner [a], E.R.F. Winter [a,1], R. Viskanta [b,*]

[a] *Lehrstuhl C für Thermodynamik, Technische Universität München, D-85747 Garching, Germany*

[b] *Heat Transfer Laboratory, School of Mechanical Engineering, Purdue University, West Lafayette, IN 47907-1288, USA*

Received 12 September 2001; received in revised form 16 April 2002

Abstract

The current contribution describes the experiments performed in an outdoor test stand for so called "double-skin-façades" at the Technical University of Munich. The purpose of the investigation was to determine the time and local averaged overall heat transfer coefficients for solar radiation augmented turbulent mixed convection flows in transparent vertical channels. The external plate of the vertical channel is formed with horizontally oriented ventilation gratings in the external glass façade, thus providing openings for the air circulation within the gap. In the course of the research, the distance between the external and the internal glass façade was measured for three gaps of 0.3, 0.6 and 0.9 m wide. Using the pressure compensation method, the effective mass flow rates for a given box-window, which is the smallest functional unit of all known double-skin-façade systems, was measured by means of a ventilation duct installed at the outlet of such a box-window. Finally, the experimental data was reduced in terms of an average Nusselt number as a function of an average Archimedes number for several gap distances.

1. Introduction

In recent years there has been erected in Central Europe an ever increasing number of office and commercial buildings distinguished by natural ventilation systems. A key feature of these novel ventilation concepts are so called "double-skin-façades" provided with adequate openings in the external façade and regular windows in the building bound façade [1]. The development of such façade systems was actually given rise to the well known "sick-building-syndrome" [2] occurring in most of fully air-conditioned high-rise buildings. Due to insufficient maintenance of the heating ventilation and air-conditioning (HVAC) systems of conventional office buildings, occupants are faced, for example, with nausea, headache and irritation of mucous membranes. Especially in Central Europe occupants of conventional office buildings have demanded individual base control over the room climate by access to windows. Extremely high wind pressure in upper floors actually prevent the realization of conventional façade systems with natural ventilation concepts. An installation of a second transparent façade in front of the building with horizontal ventilation gratings (see Fig. 1) enables one to reduce the effects of pressure fluctuation and to enable natural ventilation by opening the windows at wind speeds up to 10 m/s. This is accompanied by a decrease in operating time of the mechanical ventilation systems and reduced cooling loads compared to façade systems with indoor shading devices. The classification of double-skin-façade systems, depending on the compartmentalization of the gap between external and internal façade, and the arrangement of the ventilation gratings as well as a discussion of its advantages and disadvantages for the HVAC concepts of the buildings is detailed elsewhere [3].

In constructed buildings the distance of the gap between the transparent façade varies from 0.3 to 1.5 m resulting in aspect ratios based on a typical storey height

* Corresponding author. Tel.: +1-765-494-5622/5632; fax: +1-765-494-0539.

E-mail address: viskanta@ecn.purdue.edu (R. Viskanta).

[1] Deceased

0017-9310/02/$ - see front matter
PII: S0017-9310(02)00160-6

Nomenclature

A_b	cross-sectional area of the gap (m^2)
A_{eff}	effective area for convective heat transfer in the box window (m^2)
$\overline{Ar}_L$	average Archimedes number referred to a characteristic length (–)
c_p	specific heat capacity (J/kgK)
$\dot{G}$	solar irradiation (W/m^2)
g	gravitational acceleration (m/s^2)
H	height of the box window (m)
$h_{in/out}$	height of the air inlet and outlet, respectively (m)
L	characteristic length (m)
$\dot{M}$	mass flow rate in (kg/s)
$\overline{Nu}_L$	average Nusselt number referred to a characteristic length (–)
S	distance between external and internal façade (m)
T_∞	outdoor temperature
$\overline{T}_b$	mean bulk temperature in the box-window (K)
$\Delta\overline{T}_{GA}$	difference between mean glass surface temperature and air temperature (K)
ΔT_{out-in}	difference between air temperatures at the out- and inlet (K)
$\bar{v}_b$	is the vertical component of the bulk velocity (m/s)
x	local horizontal coordinate starting at the internal facade
$\bar{\alpha}$	average overall mean heat transfer coefficient (W/m^2 K)
β	thermal expansion coefficient (1/K)
λ	thermal conductivity of air (W/mK)
$\rho_{\overline{T}_b}$	air density at $\overline{T}_b$ (kg/m^3)

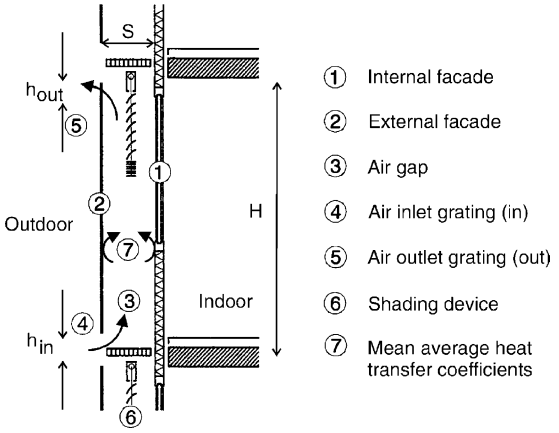

Fig. 1. Schematic diagram of a double-skin-façade according to Faist [6].

of about 4 m of $3 < H/S < 15$. Depending on the compartmentalization of the spacing the aspect ratio, B/S varies in a range of 0.5–500.

A comprehensive literature survey of mixed convection between vertical parallel plates provided by Fedorov and Viskanta [4] showed that most of the research done in the past for electronic cooling applications has treated heat transfer by natural convection in narrow gaps between cooling fins. This work was mainly theoretical in nature and is mostly focused on laminar flow situations. Furthermore, the influence of a horizontal air entrance was not investigated in the published studies.

The research initiated by the European façade industry has mainly focused on effective air exchange rates within the rooms attainable by the application of different double-skin-façades in front of the building [5]. Only in a few cases an attempt was made to predict the increase in air temperature within the gap subjected to ambient conditions and geometry of the double-skin-façades [6,7]. A broad, but superficial review of the technical aspects to be considered in designing double-skin-façades has recently been provided by Oesterle et al. [8].

The fluid flow in transparent vertical open gaps of double-skin-façades is caused by solar irradiation and strong fluctuating dynamic wind forces of different directions and intensity, depending on the façade segment considered (height and orientation) of the building. However, in the present investigation the experimental outdoor facility was designed in order to eliminate the influence of the wind forces, and heat transfer rates were, therefore, studied only for solar radiation induced turbulent mixed convection flows. Theoretically, the flow regime in the box-window may be divided into free convection within a channel formed by two vertical plates or in a rectangular duct superimposed by forced convection due to a chimney effect, depending on the dimensions of the gap and the solar irradiation. In the experimental apparatus the influence of shading structures installed in the gap of constructed double-skin-façades was neglected. As a result, all experiments were conducted without the activated shading device. Furthermore, the windows of the internal façade were kept closed and the physical and radiative properties of the glazings were not varied.

The experiments were conducted in order to validate a theoretical model for steady two-dimensional incom-

pressible turbulent mixed convection flow in a transparent channel based on an analysis published by Fedorov et al. [4,9] and Mohamad and Viskanta [10]. A low-Reynolds k–ε turbulence model was adopted using constants and wall damping functions for forced convection boundary layer flows reported by Launder [11] and already applied successfully for natural convection flows by Fedorov et al. [4,9]. A control volume, finite-difference numerical integration technique was used to solve the equations with appropriate boundary conditions. The SIMPLER algorithm is employed to numerically integrate the model equations in primitive or dimensional variables. The method of solution is detailed elsewhere [10] and needs not to be repeated here. The degree of uncertainty in the predicted results amounts to less than 10% in comparison to the experimental results.

2. Experiments

Most of the experiments reported in the European literature were conducted at indoor facilities using artificial radiation sources [7] and, in general, small scale test façades [5]. For the experiments reported here a South oriented outdoor test stand, shown in Fig. 2, was designed and built on top of a unit of the new Mechanical Engineering Faculty Building of the Technical University Munich in Garching. The design of the test facility allows to simulate a representative unit of all known double-skin-façade systems of a maximum width of 3 façade subunits (0.90 m each) and a height of one or two storeys, though only for the ground floor the interaction between the ventilated air gap and an adjacent test room of 4×2 m is feasible.

Table 1
Dimensions (in m) of the outdoor teststand for double-façade systems

	S	H	B	h
Minimum	0.3	2.4	0.9	0.01
Maximum	1.2	4.8	2.7	0.3

One of the key features of the test stand is its extreme geometric flexibility allowing to vary the distance between the external and internal façade S, the total height H, and the width B, as well as the height of the horizontal ventilation gratings $h_{\mathrm{in/out}}$ according to Table 1.

The experiments were performed using a single box-window representing the smallest functional subunit of all double-skin-façade systems. To determine the effective overall heat transfer coefficients for a sole box-window unit the mass flow rate under natural convection conditions had to be measured. This was accomplished by using the pressure compensation method reported in Refs. [12,13]. To this purpose, the box-window was provided by a ventilation duct with a Venturi section for measuring the flow velocity and temperature of the air in order to compute the mass flow rate (compare Fig. 2). By means of a frequency controlled fan at the air exit of the duct, the mass flow was regulated in such a way that the difference of the static pressure at the outlet of the box window, recorded right after the outlet grating, and the ambient static pressure (measured at an appropriate place characterized by calm outdoor conditions) was adjusted to a vanishingly small value. As a result, the static pressure at the outlet of the inside duct was always connected with the ambient static pressure, and the mixed convection flow in the box window was not influenced neither by the rotational speed of the fan

Fig. 2. Outdoor test facility for double-skin-façade systems.

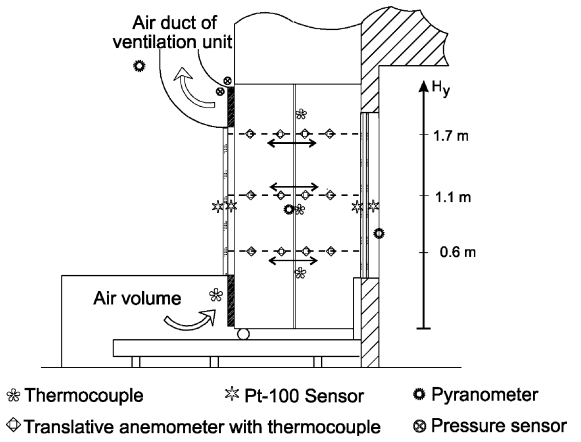

Fig. 3. Measurement positions in the box-window.

at the end of the duct nor by the fluctuating wind loads subjected by the outdoor teststands. In order to eliminate the influence of the dynamic wind forces on the fluid flow also at the air-inlet, additionally a wooden crate measuring three times the volume of the box-window unit was built in front of it (compare Figs. 2 and 3).

Surface temperatures at locations shown in Fig. 3 were measured with resistance thermometer (PT100) and air temperatures by means of thermocouples (type K). Each channel of the data logger was calibrated by means of a thermostat and calibration thermometers in a range of 0–50 °C to obtain the utmost precision in surface and air temperature measurements. Impeller wheel (plate) thermal anemometers (velocity range 0.05–1.0 m/s), scanning the distance between external and internal façade, were installed along the height of the box-window unit in order to determine two dimensional temperature and velocity fields in the gap. The air velocity was measured with a frequency of 20 Hz and an integration time of 2 min based on time-averaged sensor internal values recorded with a sampling interval of 1 s. Due to the influence of air temperature (T_A) within the façade upon the precision of the sensor, the accuracy varied between ±3 (for $T_A = 20$–26 °C) and ±13% (for $T_A \approx 45$ °C). The velocity sensors were calibrated in the measurement environment with a software integral and automated calibrator provided by the manufacturer. Furthermore, ambient conditions such as solar irradiation on the South oriented façade, wind speed and direction as well as atmospheric conditions were also recorded. The details are described elsewhere [3].

2.1. Description of experiments

During an almost year-long experimental study two types of experiments were carried out. The first test series was conducted under mixed convection conditions, whereas in other series forced convection flow was investigated by adjusting the mass flow rates from 0.06 to 0.6 kg/s. By this means, subject to the geometry of the gap and the air in- and outlet temperature, overall average heat transfer coefficients were determined. The optimum mass flow rates were characterized by a maximum increase of the air temperature in the gap of 2 K. The results of all test series are detailed in Ref. [3]. For the sake of clarity, in the following only the results for mixed convection are summarized.

All experiments under mixed convection conditions were performed at high-noon. The number of measuring points along the translating thermal anemometers was limited to 30, thus allowing to complete an experiment within 1 h by recording every 2 min mean values at each position of the two-dimensional grid. The nonuniform grid was characterized by a high resolution on both sides of the channel. A sufficiently high air inlet volume (Fig. 3) and the ventilation duct yielded pseudo-steady-state conditions. Surface and air temperatures used for the calculation of the average overall heat transfer coefficients were based on hour-long mean values, while the overall average heat transfer coefficients $\bar{\alpha}$ were obtained by equating the enthalpy balance for the air flow through the box window unit with the convective heat transfer in the gap:

$$\bar{\alpha} = (\dot{M} \times \Delta T_{\text{out-in}})/(A_{\text{eff}} \times \Delta \overline{T}_{\text{GA}}) \tag{1}$$

where $\dot{M}$ is the mass flow rate in kg/s, $\Delta T_{\text{out-in}}$ is the temperature difference between outlet and inlet in (K), A_{eff} is the effective area for convective heat transfer exchange in the box window in (m^2) and $\Delta \overline{T}_{\text{GA}}$ is the temperature difference between arithmetic mean temperature of surrounding glass sheets and average air temperature of the box-window in (K).

Depending on the aspect ratio H/S, the area and the temperature of the vertical glass sheets closing the box-window unit on both sides were taken into consideration or were neglected. Although the surface area increases with decreasing H/S values, flow visualization and the interpretation of the horizontal and vertical velocity and temperature profiles showed that its effects on convective heat transfer were only of minor nature.

In dimensionless form, the average overall mean heat transfer coefficient $\bar{\alpha}$ is given in terms of an average Nusselt number $\overline{Nu}_L$ as a function of an average Archimedes number $\overline{Ar}_L$ with the following definitions,

$$\overline{Nu}_L = \frac{\bar{\alpha}_L L}{\lambda_{\overline{T}_b}} \tag{2}$$

where L is the characteristic length and λ is the thermal conductivity of air evaluated at the mean bulk temperature $\overline{T}_b$ in the box-window. The average Archimedes number is defined as

Table 2
Ranges of experimental uncertainty for the experimental key values

Measured quantity	Range of measurement uncertainty
Mass flow rate ($\dot{M}$)	±0.5–2%
Temperature differences ($\Delta\overline{T}$)	±0.1–0.3 K
Specific heat capacity (c_p)	±0.2–0.5%
Heat exchanging area (A_{eff})	±0.5–1.0%

$$\overline{Ar}_L = \frac{gL\beta\Delta\overline{T}}{\overline{v}_b^2} = \left(\frac{gL\Delta\overline{T}_{GA}}{\overline{T}_b}\right)\left(\frac{A_b^2\rho_{\overline{T}_b}^2}{\dot{M}^2}\right) \quad (3)$$

where g is the gravitational acceleration, β is the thermal expansion coefficient, $\overline{v}_b$ is the vertical component of the bulk velocity in (m/s) and A_b (m^2) is the area of the cross-sectional view of the gap.

Using the height of the gap H as the characteristic length of the system, the effective heat transfer area A_{eff} is calculated only by means of the transparent areas of the external and internal façade (model of mixed convection on a "vertical plate"—in the following is called "plate-model"). On the other hand, for mixed convection flow in a "vertical channel" (in the following called "channel-model") the hydraulic diameter D_h has to be used as the characteristic length, resulting in a larger effective heat transfer area A_{eff} because all four walls of the channel are considered in Eq. (1). The calculation of the mean surface temperature $\overline{T}_G$ of the heat transferring surface (panes) necessary for the determination of the mean temperature difference $\Delta\overline{T}_{GA}$. All surface temperatures of the channel are considered for the averaging in case of the channel-model and only the surface temperatures of the internal and external façade in case of the plate-model.

The estimation of the experimental uncertainty is based on Eq. (1) and the ranges of experimental uncertainty of the key quantities given in Table 2 were used.

The estimated experimental uncertainties of the computed overall mean heat transfer coefficients according to Eq. (1) averaged 4–7% (optimistic estimation) for summer conditions subject to the temperature difference $\Delta\overline{T}_{GA}$, whereas pessimistic assumptions resulted in uncertainties of 12–17%. Due to higher temperature differences in the winter, the experimental uncertainty decreases so the lower bound of the given ranges becomes appropriate.

3. Results

3.1. Temperature and velocity profiles

In the following figures typical horizontal velocity and temperature profiles for distances of $S = 0.33$ m ($H/S \approx 8$) between the external and internal façades and a height of the air inlet and outlet of $h_{in/out} = 0.04$ m for mixed convection are presented. Ambient conditions for a typical summer season on a south-bound façade in Central Europe were measured with solar irradiation of $\dot{G} = 530$ W/m^2 and air temperature of $T_\infty = 25$ °C, resulting in a mean mass flow rate of $\dot{M} \approx 0.015$ kg/s in the box-window. This air flow rate was induced by mean temperature differences between the surface of the panes and the bulk air temperature of about 6–8 K. An examination of Figs. 4 and 5 reveals that the air gap may be subdivided into four seperate flow regimes adjacent to the external façade ($0 < x/S < 0.2$) and a main flow zone characterized by the steepest gradients of vertical air velocity. This holds especially true in the first third of the height of the box window (compare the curve for $h_y = 0.6$ in Fig. 4 with the almost constant temperature

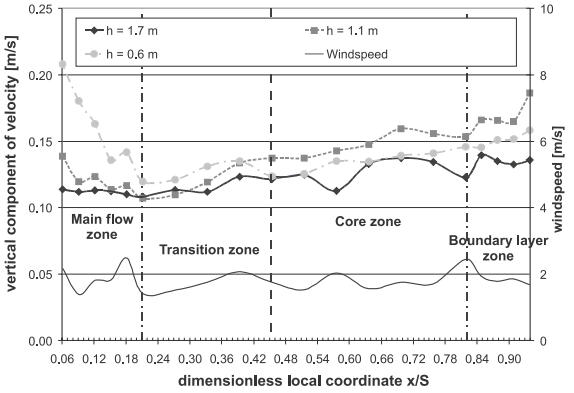

Fig. 4. Vertical components of velocity as a function of dimensionless local coordinate x/S in a gap of $S = 0.33$ m ($S/H = 8$) and $h_{in/out} = 0.04$ m together with the mean wind velocity.

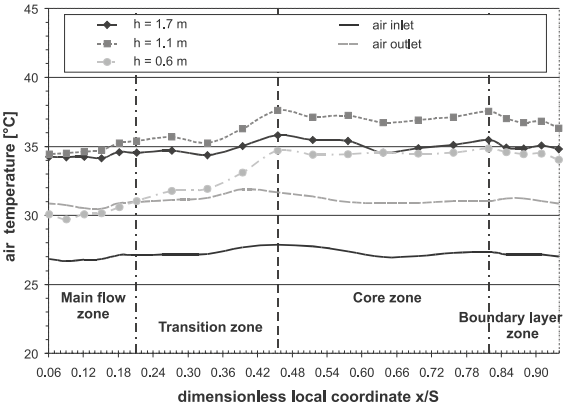

Fig. 5. Air temperature as a function of dimensionless local coordiante x/S in a gap of $S = 0.33$ m ($S/H = 8$) and $h_{in/out} = 0.04$ m together with the mean temperature at the air inlet and outlet.

profiles in Fig. 5). The main flow zone is followed by a transition zone characterized by the highest gradients in the course of the temperature profile. For values of the dimensionless local coordinate x/S ($0.46 < x/S < 0.82$) a core zone may be identified by the highest constant air temperatures in each of the three measuring planes. This core zone has only a minor influence upon the air exchange rate of the box window compared to those rates occurring in the main flow zone next to the internal façade. The flow zone situated immediately adjacent to the external pane and generally having higher surface temperatures (not shown here) than the internal pane is responsible for the development of a boundary layer and subsequent higher air exchange rates and again decreasing air temperatures. This effect is caused by a downward directed flow as a result of a quite large flow resistance at the outlet of the air gap using a grating with $h_{\mathrm{in/out}} = 0.04$ m.

3.2. Mass flow rates

As already mentioned, the mass flow rate for mixed convection was measured using the pressure compensation method. In the following figures the mass flow rate is plotted versus the mean temperature difference between the pane surface and the bulk air temperature for different heights of inlet and outlet gratings ($h = 0.04$, 0.15, 0.30 m) for a gap distance of $S = 0.33$ and 0.93 m in Figs. 6 and 7, respectively. For a gap with a distance $S = 0.33$ m the channel mode was used to determine the mean surface temperatures, whereas for a gap with $S = 0.93$ m the plate model was adopted. Although the area of the vertical lateral faces of the box-window is becoming larger for higher values of the gap distance S, nevertheless the flow circulation in the box window, characterized by a very thin main flow zone at the internal façade, prevents an effective participation of these side panes in the convective heat transfer. Therefore, in this case they are not considered for the calculation of the heat exchange area A_{eff} and the mean temperature of the surrounding surfaces.

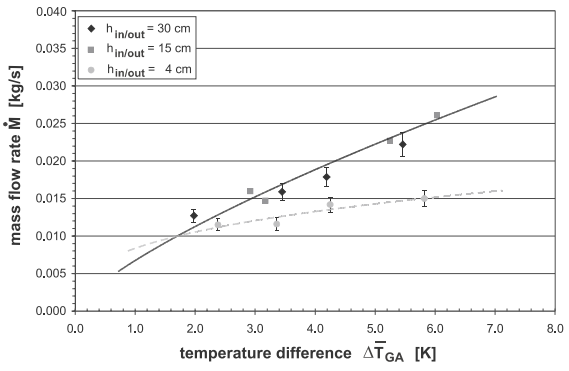

Fig. 6. Mass flow rates $\dot{M}$ for turbulent mixed convection in a box-window with a gap of $S = 0.33$ m and the curves represent experimental trends.

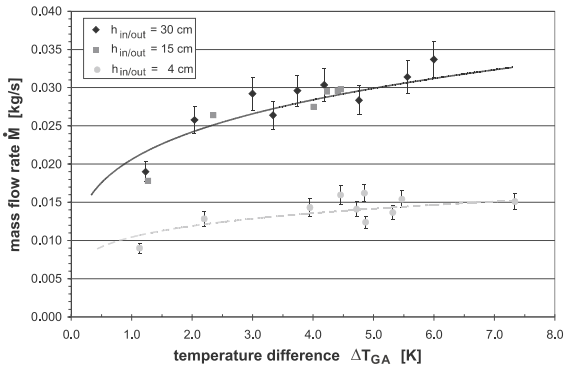

Fig. 7. Mass flow rates $\dot{M}$ for turbulent mixed convection in a box-window with a gap of $S = 0.93$ m and the curves represent experimental trends.

It was found that a decreasing height of the gratings from $h = 0.30$ m down to 0.15 m had, in general, only small effect on the mass flow rate in the box-window. Minimizing the height of the air inlet and outlet to $h = 0.04$ m led to small mass flow rates between 0.10 and 0.15 kg/s nearly constant with an increasing gap distance (Figs. 6 and 7). The curves in the figures represent the experimental trends. For $h \geqslant 0.06$ m the influence of an increasing gap distance S is stronger for smaller temperature differences.

3.3. Average heat transfer coefficients

By means of the foregoing mass flow rates $\dot{M}$ presented, the following average Nusselt numbers $\overline{Nu}_{\mathrm{L}}$ plotted in Figs. 8 and 9 versus the average Archimedes numbers $\overline{Ar}_{\mathrm{L}}$ were calculated. Their values are based on

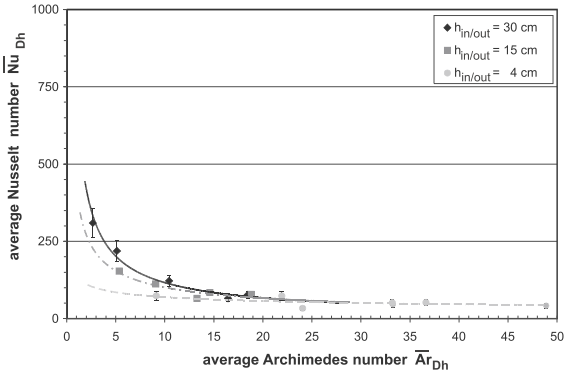

Fig. 8. Average mean Nusselt numbers as a function of the average mean Archimedes number $\overline{Ar}_{\mathrm{Dh}}$ for a gap of $S = 0.33$ m with the curves representing the experimental trends.

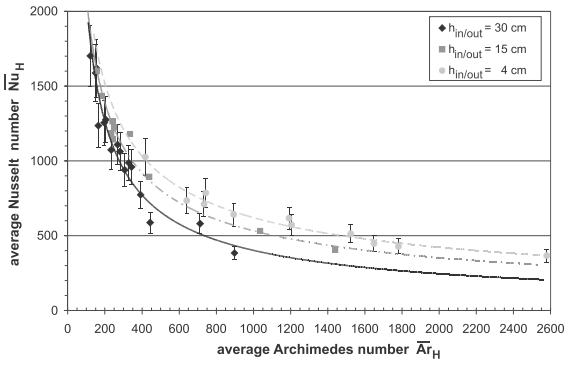

Fig. 9. Average mean Nusselt numbers as a function of the average mean Archimedes number for a gap distance of $S = 0.93$ m with the curves representing experimental trends.

time-averaged temperatures. In the analysis all panes were considered to be relevant for convective heat transfer. For a gap distance of $S = 0.33$ m the channel model was used, whereas the vertical plate model was employed for the flow in a gap with a distance of $S = 0.93$ m was treated as a mixed convection at two separate vertical plates. In case of a small air gap, the influence of the height of the inlet and outlet gratings $h_{in/out}$ was found to be almost negligible (Fig. 8).

The average Archimedes number in Figs. 8 and 9 demonstrates that free convection dominates the flow. Here, the Archimedes number $\overline{Ar}_L$ was referred to a mean air velocity in the box-window and not to local velocities in the main flow zone. This resulted in smaller values for $\overline{Ar}_L$, indicating mixed or even forced convection flow regime. In case of larger air gap distances ($S > 0.6$ m) the impact of the height of the inlet and outlet gratings becomes significant. As a consequence of higher air velocities at the inlet grating for $h_{in/out} = 0.04$ m, the heat transfer rate increases. For higher Archimedes numbers at a maximum height of $h_{in/out} = 0.3$ m leads to a decrease of about 30% in the Nusselt numbers compared to the value for the minimum height of $h_{in/out} = 0.04$ m.

4. Conclusions

The experimental and theoretical studies yielded the following results:

- Solar radiation induced mixed convection fluid flow in double-skin-façades depends very strongly on the aspect ratios H/S, H/h and S/h.
- Depending upon the air velocity in the entrance grating which is influenced by the height of the grating $h_{in/out}$ and the height of the box-window H, a more or less highly circulating flow with an upwards directed flow close to the internal façade and a downwards directed flow adjacent the external façade are induced.
- Due to the circulatory motion of the flow the highest temperatures do not occur at the outlet of the box-window but in the core of the air gap.
- The gap may be divided in most of the cases of practical interest into four seperate flow zones: a main flow zone adjacent to the internal façade, followed by a transition and core zone, and finally a boundary layer zone adjacent to the external façade.
- Turbulent mixed convection in air gaps with a distance of $S < 0.6$ m, should be analyzed using the "channel model" for the computation of the average Nusselt number as a function of the average Archimedes number, whereas the "plate model" has to be employed for situations within an air gap of distances of $S > 0.6$ m.

At locations different from those where the experiments were conducted, both higher solar radiation and lower outdoor temperatures than those presented in the paper have to be considered. This is expected to result in higher average mean Nusselt numbers due to higher mass flow rates and different flow structures, but always yielding the same qualitative dependence on the geometrical parameter ratios of the box-window identified. Detailed parameter analysis for a box-window of typical geometry ($H = 2.4$ m, $S = 0.6$ m and $h = 0.1$ m) with a solar irradiation of about 600 W/m^2 and a decrease in outdoor temperature from 26 °C down to 5 °C yielded, for example, an increase in the average mean Nusselt number of about 20%. Whereas, an increase in the solar irradiation from 500 to 900 W/m^2 resulted in an increase in the average mean Nusselt number of about 25%.

References

[1] A. Compagno, Intelligent Glass façades—Material Practice Design, Birkäuser Publishers, Basel, 1999.
[2] P. Kröling, Sick Building Syndrom, in: Phillipp Oswalt (Ed.), Wohltemperierte Architektur, C.F. Mueller Verlag, Heidelberg, 1995, pp. 84–87.
[3] A. Zöllner, Experimentelle und theoretische Untersuchung des kombinierten Wärmetransports in Doppelfassaden, Doctoral Dissertation, Technical University of Munich, Garching, Germany, 2001.
[4] A.G. Fedorov, R. Viskanta, Turbulent natural convection heat transfer in an asymmetrically heated vertical parallel-plate channel, Int. J. Heat Mass Transfer 40 (16) (1997) 3849–3860.
[5] C. Ziller, Modellversuche und Berechnungen zur Optimierung der natürlichen Lüftung durch Doppelfassaden, Doctoral Dissertation, Rheinisch Westfälisch Technische Hochschule (RWTH), Aachen, Germany, 1999.
[6] A.P. Faist, La Facade double-peau, Report of the Ecole Polytechnique Federal (EPF) de Lausanne, Lausanne, CH, 1998.

[7] K. Doege, U. Franzke, Zusammenwirken von Außenklima, Doppelfassade und Raumklima, Technik am Bau 28 (1998) 41–46.
[8] E. Oesterle, M. Lutz, R.-D. Lieb, W. Heusler, Doppelschalige Fassaden—Ganzheitliche Planung, Callwey-Verlag, München, 1999.
[9] A.G. Fedorov, R. Viskanta, A.A. Mohamad, Turbulent heat and mass transfer in an asymmetrically heated vertical parallel-plate channel, J. Heat Fluid Flow 8 (1997) 307–315.
[10] A.A. Mohamad, R. Viskanta, Application of low-Reynolds number k–ε Turbulence model to buoyant and mixed flows in a shallow cavity, Fundamentals of Mixed Convection, HTD vol. 213, ASME, New York, 1992, pp. 43–54.
[11] B.E. Launder, On the computation of convective heat transfer in complex turbulent flows, J. Heat Transfer 110 (4B) (1988) 1112–1128.
[12] H. Presser, Volumenstrommessung an Luftdurchlässen nach dem Kompensations-verfahren, Heizung-Lüftung/Klima-Haustechnik 29 (2) (1978) 59–68.
[13] H. Bittner, R. Detzer, Luftstrommessung am Auslaß mit der Nulldruckmethode, Klima-Kälte Heizung 10 (1974) 425–428.